



## Article

# Study of the Structural, Optical and Strength Properties of Glass-like $(1-x)\text{ZnO}-0.25\text{Al}_2\text{O}_3-0.25\text{WO}_3-x\text{Bi}_2\text{O}_3$ Ceramics

Artem L. Kozlovskiy <sup>1,2,\*</sup> , Aibek S. Seitbayev <sup>1,2</sup>, Daryn B. Borgekov <sup>1,2</sup> and Maxim V. Zdorovets <sup>1,2</sup> <sup>1</sup> Laboratory of Solid State Physics, The Institute of Nuclear Physics, Almaty 050032, Kazakhstan<sup>2</sup> Engineering Profile Laboratory, L.N. Gumilyov Eurasian National University, Astana 010008, Kazakhstan

\* Correspondence: kozlovskiy.a@inp.kz; Tel./Fax: +7-7024413368

**Abstract:** The main purpose of this work is to study the effect of substitution of zinc oxide for bismuth oxide in the composition of  $(1-x)\text{ZnO}-0.25\text{Al}_2\text{O}_3-0.25\text{WO}_3-x\text{Bi}_2\text{O}_3$  ceramics, as well as the accompanying processes of phase transformations and their influence on the optical and strength properties of ceramics. The use of these oxide compounds as materials for creating shielding coatings or ceramics is due to the combination of their structural, optical, and strength properties, which make it possible to compete with traditional protective glasses based on rare earth oxide compounds. Interest in these types of ceramics is due to their potential for use as basic materials for shielding ionizing radiation as well as for use as radiation-resistant coatings. The main research methods were X-ray diffractometry to determine the phase composition of ceramics; scanning electron microscopy and energy dispersive analysis to determine the morphological features and isotropy of the distribution of elements in the structure; and UV-V is spectroscopy to determine the optical properties of ceramics. During the studies, it was found that an increase in the  $\text{Bi}_2\text{O}_3$  concentration leads to the formation of new phase inclusions in the form of orthorhombic  $\text{Bi}_2\text{WO}_6$  and  $\text{Bi}_2\text{W}_2\text{O}_9$  phases, the appearance of which leads to an increase in the density of ceramics and a change in the dislocation density. An analysis of the strength properties, in particular, hardness and crack resistance, showed that a change in the phase composition of ceramics with an increase in the  $\text{Bi}_2\text{O}_3$  concentration leads to a significant strengthening of the ceramics, which is due to the effect of the presence of interfacial boundaries as well as an increase in the dislocation density.

**Keywords:** protective ceramics; doping; strength properties; absorption; shielding; phase transformations

**Citation:** Kozlovskiy, A.L.; Seitbayev, A.S.; Borgekov, D.B.; Zdorovets, M.V. Study of the Structural, Optical and Strength Properties of Glass-like  $(1-x)\text{ZnO}-0.25\text{Al}_2\text{O}_3-0.25\text{WO}_3-x\text{Bi}_2\text{O}_3$  Ceramics. *Crystals* **2022**, *12*, 1527. <https://doi.org/10.3390/cryst12111527>

Academic Editors: Yu-Chen Liu and Yu-Ze Chen

Received: 16 October 2022

Accepted: 25 October 2022

Published: 27 October 2022

**Publisher's Note:** MDPI stays neutral with regard to jurisdictional claims in published maps and institutional affiliations.



**Copyright:** © 2022 by the authors. Licensee MDPI, Basel, Switzerland. This article is an open access article distributed under the terms and conditions of the Creative Commons Attribution (CC BY) license (<https://creativecommons.org/licenses/by/4.0/>).

## 1. Introduction

The general concept of protection against ionizing radiation, as well as its negative impact, implies the creation and use of such protective materials that are able to absorb ionizing radiation with maximum efficiency and minimize the impact of radiation on the environment or living organisms [1–3]. Conventional protection methods used almost universally include the use of shielding protective materials, such as lead, taped glass, concrete or borated polymer [4,5]. All of these materials have very good shielding characteristics and have performed reasonably well in many industries that use ionizing radiation or sources of ionizing radiation [6–8].

However, despite the widespread use of traditional protective shielding materials, an increase in the widespread use of ionizing radiation sources, including as energy sources, requires radically new solutions and materials in this direction [9,10].

Over the past few years, research has been actively conducted in this direction, associated with both the theoretical and practical development of compositions of new types of protective materials based on oxide compounds of refractory and rare earth elements [11–15]. Interest in these types of compounds is due to the combination of their physicochemical, strength, optical, and absorbing properties, the variation of which makes it possible to obtain materials with different shielding efficiencies. A great contribution to

this direction was made by the scientific group led by Sayyed M.I., which in a number of works showed a high level of promise for the use of multicomponent oxide ceramics and glasses as protective shielding materials [16–20]. At the same time, according to a number of authors, the search for the optimal compositions of protective materials is still far from complete due to the large number of possible variations as well as the expansion of the range of practical applications of ionizing radiation.

Glasses and ceramics based on ZnO, WO<sub>3</sub>, and Al<sub>2</sub>O<sub>3</sub> compounds, which are of interest due to their physicochemical, structural, optical, and absorption properties, have been some of the promising materials for shielding in the past few years [21–23]. A feature of these compounds is the presence of the formation of structures of the type of complex oxides of ZnWO<sub>4</sub> and ZnAl<sub>2</sub>O<sub>4</sub>, the formation of which leads to an increase in the absorbing and shielding ability of materials as well as their strength characteristics. For example, it was shown in [21] that the obtained structures based on compounds of the ZnO-WO<sub>3</sub>-La<sub>2</sub>O<sub>3</sub>-Al<sub>2</sub>O<sub>3</sub> type have a high thermal stability depending on the degree of crystallization. In [22], it was shown that the partial replacement of zinc and lead oxides with the WO<sub>3</sub> compound leads to an increase in the absorbing capacity of glass ceramics. The processes of glass formation, as well as the stability of structural properties for structures containing zinc oxide, were studied in detail in [23]. Unlike telluride or lead glasses or ceramics, developments in the field of creating glass ceramics based on ZnO, WO<sub>3</sub>, Al<sub>2</sub>O<sub>3</sub> compounds have a number of significant advantages. These advantages primarily consist of optical and absorption characteristics as well as higher strength properties. At the same time, the cost of the initial components for the manufacture of glass ceramics based on ZnO, WO<sub>3</sub>, and Al<sub>2</sub>O<sub>3</sub> is significantly lower than that of telluride or lead glasses, for which the cost of rare earth oxide compounds is much higher.

At the same time, much attention has recently been paid to research related to various methods of modifying zinc-containing glass ceramics, the main purpose of which is to increase both the resistance of these ceramics to external influences and the shielding characteristics. In most cases, the doping of glasses to ceramics leads to an acceleration of the phase formation or glass transition processes, which makes it possible to lower the sintering or fusion temperature, as well as increasing strength and hardness. As a rule, Bi<sub>2</sub>O<sub>3</sub> or Y<sub>2</sub>O<sub>3</sub> are used for such purposes, which are very promising compounds for these purposes.

The aim of this work is to study the effect of the phase composition of synthesized ceramics based on (1-x)ZnO-0.25Al<sub>2</sub>O<sub>3</sub>-0.25WO<sub>3</sub>-xBi<sub>2</sub>O<sub>3</sub> compounds and their variations, as well as establishing the dependence of the effect of the phase composition on the optical and strength characteristics of ceramics.

Interest in these ceramics is due to the prospect of using them as protective materials for shielding gamma, electron and neutron radiation, as well as the creation of alternative materials in the field of protective materials. In turn, the substitution of ZnO with a Bi<sub>2</sub>O<sub>3</sub> dopant will increase the density of ceramics, as well as increasing the rate of phase formation processes, and increase resistance to mechanical stress.

The relevance of this study consists in the creation of new types of shielding protective ceramics that can compete with telluride and lead glasses, which are one of the candidate protective materials. The use of new types of shielding materials will expand the range of their practical application, as well as increasing the effectiveness of protection against the negative effects of ionizing radiation.

## 2. Experimental Part

The synthesis of ceramics of the (1-x)ZnO-0.25Al<sub>2</sub>O<sub>3</sub>-0.25WO<sub>3</sub>-xBi<sub>2</sub>O<sub>3</sub> type was carried out using the method of mechanochemical synthesis by grinding oxide compounds in a given molar ratio in a planetary mill and subsequent thermal annealing in a muffle furnace at a temperature of 1100 °C for 5 h. The samples were obtained by the standard method of sintering and subsequent air quenching when removing the samples from the furnace.

The elemental composition was measured, and the surface of the samples was mapped using the energy dispersive analysis method implemented using an Oxford Instruments (Bruker, Berlin, Germany) detection system built into a Hitachi TM3030 scanning electron microscope (Hitachi, Tokyo, Japan).

Table 1 presents data on the composition and content of the initial oxide compounds used for the synthesis of  $(1-x)\text{ZnO}-0.25\text{Al}_2\text{O}_3-0.25\text{WO}_3-x\text{Bi}_2\text{O}_3$  ceramics as well as a brief designation of the samples for a more convenient interpretation of the obtained dependences. The variation of the oxide components was carried out by replacing zinc oxide with bismuth oxide in the range of 0–0.25 mol. The choice of this variation is due to the properties of  $\text{Bi}_2\text{O}_3$ , which make it possible to accelerate the processes of phase formation during thermal sintering, as well as increasing the strength characteristics of glasses.

**Table 1.** Data on the compositions of ceramics used for synthesis.

Sample	$(1-x)\text{ZnO}-0.25\text{Al}_2\text{O}_3-0.25\text{WO}_3-x\text{Bi}_2\text{O}_3$			
	ZnO, mol	$\text{Al}_2\text{O}_3$ , mol	$\text{WO}_3$ , mol	$\text{Bi}_2\text{O}_3$ , mol
ZnAlWBiO-0	0.5	0.25	0.25	-
ZnAlWBiO-1	0.45	0.25	0.25	0.05
ZnAlWBiO-2	0.40	0.25	0.25	0.10
ZnAlWBiO-3	0.35	0.25	0.25	0.15
ZnAlWBiO-4	0.30	0.25	0.25	0.20
ZnAlWBiO-5	0.25	0.25	0.25	0.25

To assess the phase composition of the obtained ceramic samples depending on the composition and ratio of the components, the X-ray diffraction method was used, which was implemented on a D8 Advance Eco X-ray diffractometer (Bruker, Berlin, Germany). Diffraction patterns were obtained with Bragg–Brentano geometry in the angular range of  $2\theta = 20-80^\circ$ . A Cu- $k\lambda$  tube was used to generate X-rays with a wavelength of 1.54 Å. The detection of reflected X-rays was carried out using an Single-Shot Detector (SSD) detector.

The optical properties of the obtained ceramic samples were studied using the UV-V is spectroscopy method by taking the transmission and absorption spectra in the wavelength range of 300–1000 nm and their subsequent processing. The spectra were obtained using a Specord-250 UV spectrophotometer (Jena Analytic, Berlin, Germany). The spectra were taken with a step of 0.1 nm and a spectrum acquisition rate of 1 nm/s.

Determination of the strength characteristics of the obtained ceramics, in order to determine the effect of change in the concentration of the components on their hardening, was carried out using the method of indentation and single compression. The indentation method was used to determine the hardness of glasses as well as their resistance to softening and hardening, depending on the phase composition. The single compression method was applied to determine the resistance to cracking and establish the magnitude of the crack resistance of glasses depending on the concentration of  $\text{Bi}_2\text{O}_3$ , as well as the effect of the phase composition on strengthening.

### 3. Results and Discussion

#### 3.1. Elemental and Morphological Analysis

Table 2 presents the data on the elemental composition in samples of synthesized ceramics, obtained using the energy-dispersive analysis method and reflecting changes in the content of elements depending on the concentration of the components used for synthesis.

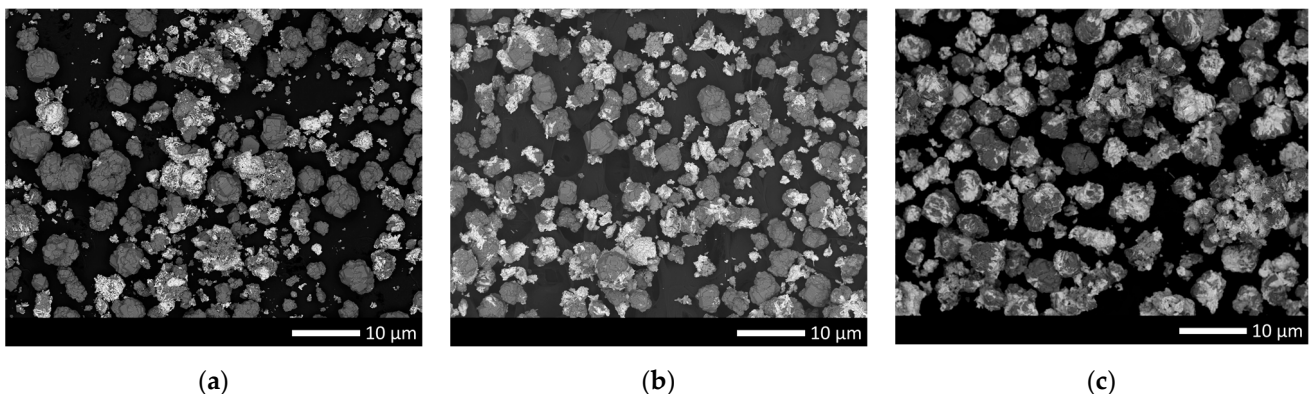
**Table 2.** Elemental composition data.

Sample	Concentration, at. %				
	Zn, at. %	Al, at. %	W, at. %	Bi, at. %	O, at. %
ZnAlWBiO-0	43.37 ± 1.45	21.34 ± 0.93	5.65 ± 0.32	-	29.64 ± 1.63
ZnAlWBiO-1	41.23 ± 1.24	20.74 ± 0.92	5.74 ± 0.45	2.56 ± 0.21	29.73 ± 1.35
ZnAlWBiO-2	40.22 ± 1.41	20.38 ± 0.75	6.12 ± 0.51	3.86 ± 0.13	29.42 ± 1.23
ZnAlWBiO-3	37.16 ± 1.42	24.38 ± 0.86	6.68 ± 0.35	5.15 ± 0.24	25.63 ± 1.24
ZnAlWBiO-4	31.37 ± 0.91	22.77 ± 0.92	6.16 ± 0.25	9.78 ± 0.32	29.92 ± 1.34
ZnAlWBiO-5	21.26 ± 0.72	22.33 ± 0.34	7.87 ± 0.32	19.97 ± 0.63	28.57 ± 1.83

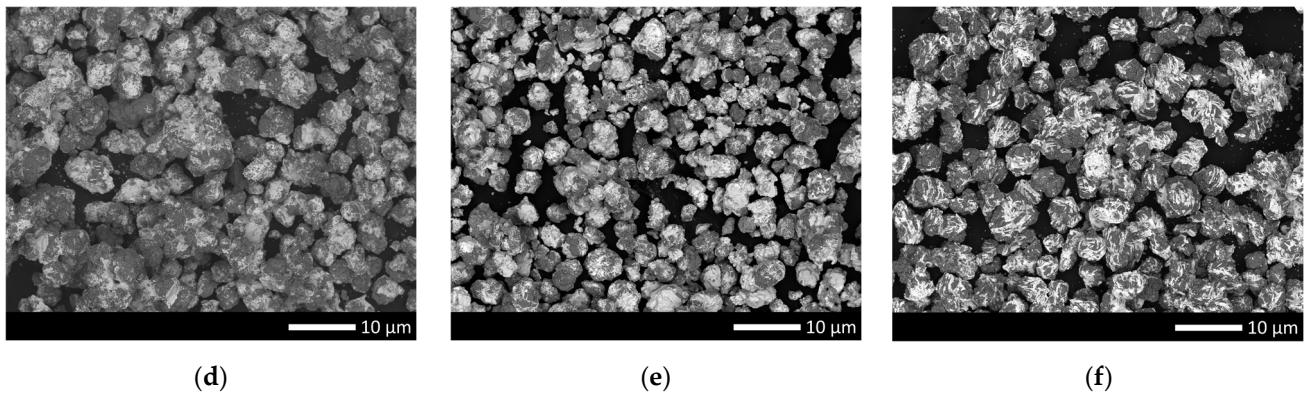
As can be seen from the presented elemental analysis data, in the case of undoped  $\text{Bi}_2\text{O}_3$  ceramics, the ratio of elements Zn:Al:W:O is 43:21:6:30, which indicates that the heavier tungsten in the synthesis process is approximately 1/10 of the zinc and aluminum components. The addition of  $\text{Bi}_2\text{O}_3$  to the composition of ceramics at low concentrations leads to an insignificant displacement of zinc due to its substitution, while the ratio of the Al and W components is within the error. A similar situation is observed for changes in the oxygen concentration. An increase in the  $\text{Bi}_2\text{O}_3$  concentration above 0.15 mol leads to a sharp decrease in the zinc content in the composition of ceramics, which may be due to the formation of new phase inclusions associated with the processes of phase transformations during thermal sintering.

Figure 1 shows the results of the morphological studies of the synthesized ceramics depending on the  $\text{Bi}_2\text{O}_3$  concentration, carried out using the method of scanning electron microscopy. The morphology was studied on synthesized powders obtained after thermal annealing. As can be seen from the data presented, the obtained ceramics are cubic or rhomboid grains, the size of which varies from 5 to 10  $\mu\text{m}$ , with a large number of various inclusions, the formation of which may be due to the formation of several phases during mechanochemical grinding and subsequent thermal annealing. At the same time, it should be noted that an increase in the  $\text{Bi}_2\text{O}_3$  concentration, according to the presented data of morphological studies, leads to the formation of feather-like or dendrite-like inclusions in large grains, which have significant differences from the basic composition of ceramics. With an increase in the  $\text{Bi}_2\text{O}_3$  concentration, there are more such inclusions, and the grain structure is close with layers or contains a large number of different veins in the form of dendrites.

Figure 2 presents the results of a detailed analysis of the mapping of ceramic samples depending on the concentration of  $\text{Bi}_2\text{O}_3$ , which reflect the distribution of elements in the composition and also allow us to evaluate the composition of newly formed inclusions in the form of dendrites or feather-like growths.

**Figure 1.** Cont.





**Figure 1.** SEM images of synthesized ceramics: (a) ZnAlWBiO-0; (b) ZnAlWBiO-1; (c) ZnAlWBiO-2; (d) ZnAlWBiO-3; (e) ZnAlWBiO-4; f) ZnAlWBiO-5.

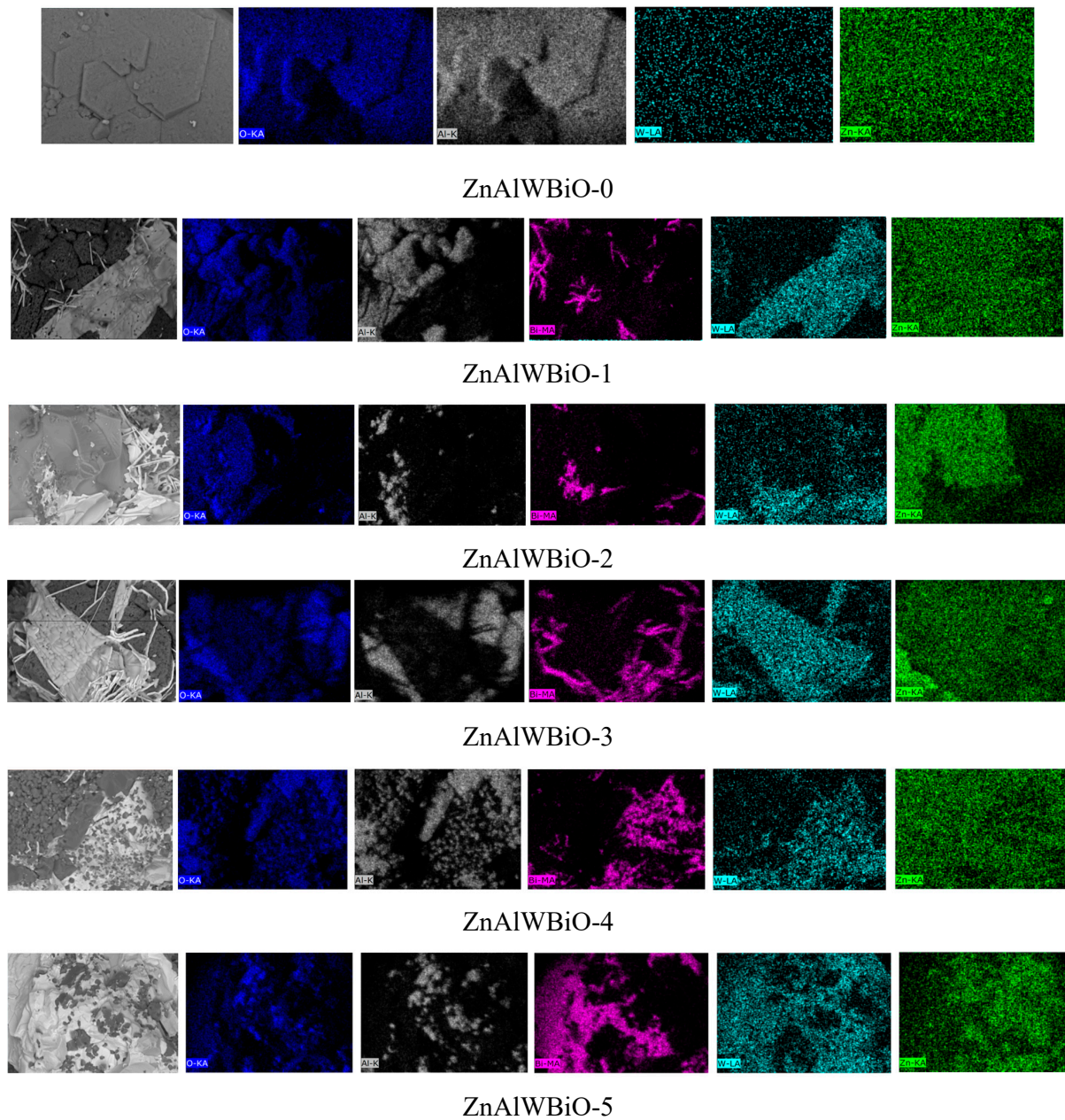


**Figure 2.** Maps of the distribution of elements in the composition of ceramics.

In the case of ZnAlWBio-0 samples that do not contain a dopant, according to the presented results of mapping the distribution of elements in the composition, it is isotropic in volume, with a predominance of zinc and aluminum. The addition of Bi<sub>2</sub>O<sub>3</sub> to the composition of ceramics, which, according to morphological studies, leads to the formation of feather-like growths or dendrites, according to mapping data, is associated with the presence of bismuth as well as a slight presence of tungsten, which may be due to the formation of structures or phases containing a mixture of these elements. An increase in the concentration of the Bi<sub>2</sub>O<sub>3</sub> dopant leads to an increase in such inclusions, as evidenced by the data of both morphological analysis and mapping results. Moreover, it should be noted that at high concentrations of the Bi<sub>2</sub>O<sub>3</sub> dopant, a detailed analysis of the morphological features shows that the grains themselves consist of two types of inclusions, which are an interstitial solid solution or a matrix of zinc, aluminum and oxygen compounds, with grains embedded in it, which are structures of the type of complex oxides containing tungsten and bismuth.

### 3.2. Phase Analysis

The analysis of the phase composition of the synthesized ceramics was carried out by comparing the positions of the experimentally obtained diffraction reflections on the diffraction patterns with the phase data taken from the database (See Figure 3). For comparison, cards from the PDF-2(2016) database were used, and the choice of the most suitable cards was based on the coincidence of the position of the lines of the PDF card with the positions of experimentally obtained diffraction reflections by more than 85–90%, taking into account structural distortions associated with the processes of phase formation during the synthesis of ceramics. The general view of the obtained diffraction patterns indicates a sufficiently high structural ordering degree of the obtained samples, which is expressed in the form and intensity of diffraction reflections as well as their deviation from the position of the reference values.

An analysis of the diffraction pattern of the ZnAlWBio-0 sample, which does not contain Bi<sub>2</sub>O<sub>3</sub>, shows that the main diffraction reflections are characteristic of the cubic phase of the spinel type ZnAl<sub>2</sub>O<sub>4</sub> and the hexagonal phase of the wurtzite type ZnO, the content of which is more than 38%. The resulting diffraction pattern also exhibits diffraction reflections characteristic of the ZnWO<sub>4</sub> monoclinic phase, the content of which is at least 22%.

Analysis of the phase composition of the samples under study, based on the obtained X-ray diffraction patterns, showed that the addition of Bi<sub>2</sub>O<sub>3</sub> to the composition of ceramics leads to the formation of new phases, which indicates the processes of phase transformations as a result of thermal sintering. In the case of adding Bi<sub>2</sub>O<sub>3</sub> in a molar content of 0.05 mol, the obtained diffraction patterns show characteristic reflections for the orthorhombic Bi<sub>2</sub>WO<sub>6</sub> phase, the content of which is at least 15%. At the same time, the content of the main ZnAl<sub>2</sub>O<sub>4</sub> and ZnO phases decreases, while the contribution of the ZnWO<sub>4</sub> phase somewhat increases (no more than 2%).

Such a change in the phase composition of ceramics upon the addition of Bi<sub>2</sub>O<sub>3</sub> can be explained by the initialization of phase formation processes associated with thermal effects. At the same time, due to the properties of Bi<sub>2</sub>O<sub>3</sub>, the phase formation processes, including the formation of structures similar to complex oxides, proceed more intensively and displace the hexagonal phase of ZnO. At the same time, analyzing the obtained data on the crystal lattice parameters, it can be seen that the displacement of the ZnO phase and an increase in the contribution of the Bi<sub>2</sub>WO<sub>6</sub> phase leads to a decrease in the crystal lattice parameters, which indicates the structural ordering of ceramics.

In the case of a Bi<sub>2</sub>O<sub>3</sub> dopant concentration of 0.15 mol in the composition of ceramics, the X-ray diffraction patterns reveal no reflections characteristic of the hexagonal ZnO phase. At the same time, an increase in the Bi<sub>2</sub>O<sub>3</sub> dopant to 0.20 mol, according to X-ray diffraction data, leads to a decrease in the contribution of the ZnWO<sub>4</sub> phase, and in the case of a Bi<sub>2</sub>O<sub>3</sub> dopant concentration of 0.25 mol, no reflections characteristic of the ZnWO<sub>4</sub>

phase are found. At the same time, X-ray reflections are observed, characteristic of the  $\text{Bi}_2\text{W}_2\text{O}_9$  orthorhombic phase, the formation of which may be due to the substitution of bismuth ions for zinc ions with a subsequent phase transformation of the  $\text{ZnWO}_4$  phase into the  $\text{Bi}_2\text{W}_2\text{O}_9$  phase or an increase in the contribution of the  $\text{Bi}_2\text{WO}_6$  phase. The absence of the  $\text{ZnWO}_4$  phase for samples with a  $\text{Bi}_2\text{O}_3$  dopant concentration of 0.25 mol is due to the processes of phase transformations associated with the displacement of this phase from the composition as well as the dominance of the  $\text{ZnAl}_2\text{O}_4$ ,  $\text{Bi}_2\text{WO}_6$  and  $\text{Bi}_2\text{W}_2\text{O}_9$  phases. Such phase transformations can be caused by a decrease in the zinc concentration, the decrease of which does not allow the formation of the  $\text{ZnWO}_4$  phase.

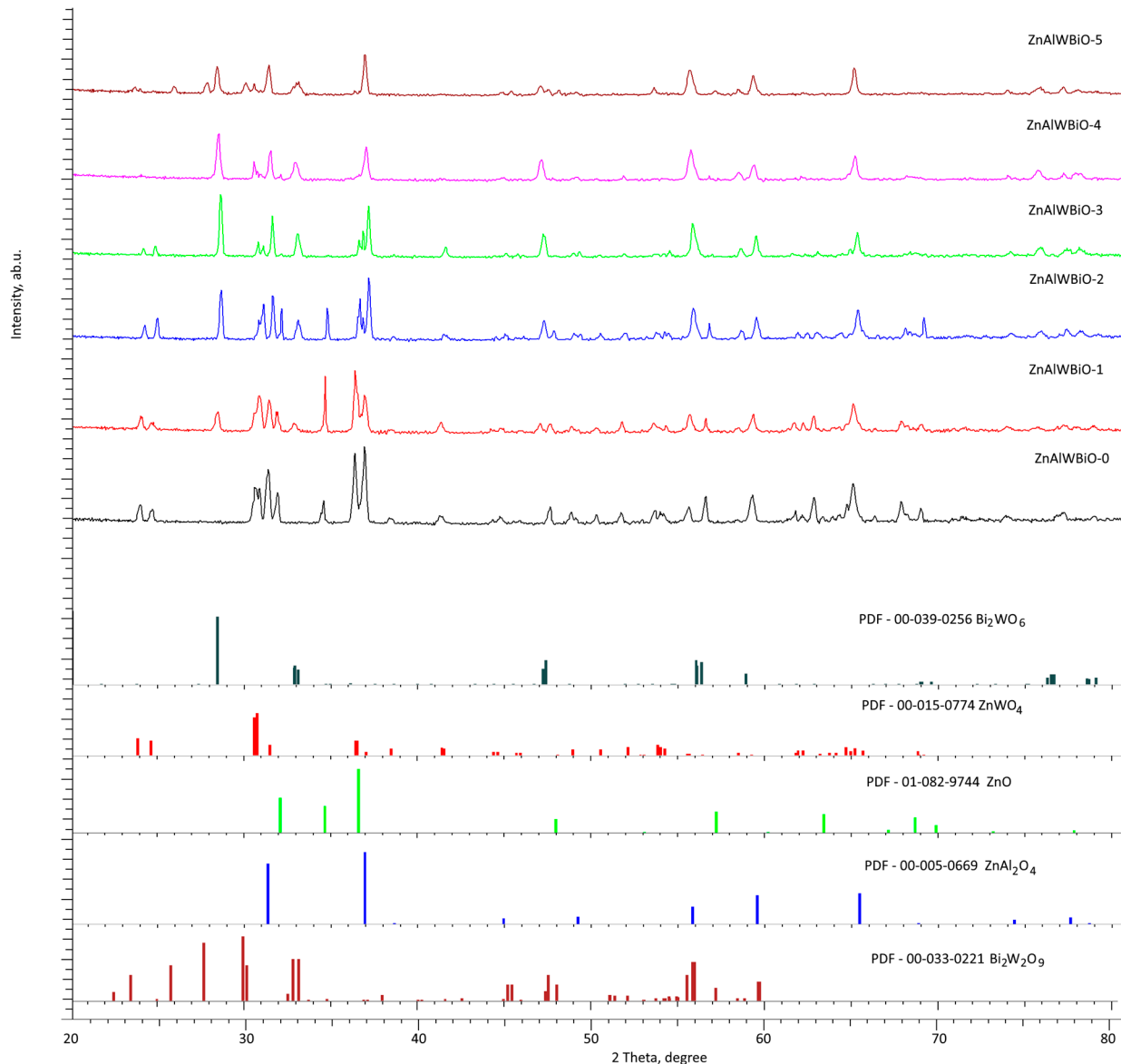


**Figure 3.** Results of X-ray diffraction of the synthesized ceramics depending on the  $\text{Bi}_2\text{O}_3$  concentration.

Table 3 presents the results of changing the parameters of the crystal lattice, obtained by analyzing the obtained diffraction patterns. The general trend of changes in the parameters of the crystal lattice has a pronounced dependence on the change in the dopant concentration, an increase in which leads to the formation of new phases. The appearance of new phases is accompanied by structural ordering, which affects the change in the parameters of the crystal lattice as well as their decrease.

Table 3. Lattice parameter data.

Sample	Lattice Parameter, Å				
	ZnO–Hexagonal P3(143)	ZnAl <sub>2</sub> O <sub>4</sub> –Cubic Fd-3 m(226)	ZnWO <sub>4</sub> –Monoclinic P2/c(13)	Bi <sub>2</sub> WO <sub>6</sub> –Orthorhombic Pbnca(61)	Bi <sub>2</sub> W <sub>2</sub> O <sub>9</sub> –Orthorhombic Pbn21(38)
ZnAlWBiO-0	a = 3.2436, c = 5.1948	a = 8.0769	a = 4.6791, b = 5.7077, c = 4.9181, β = 90.445 <sup>0</sup>	-	-
ZnAlWBiO-1	a = 3.2289, c = 5.1815	a = 8.0625	a = 4.6771, b = 5.7054, c = 4.9143, β = 90.214 <sup>0</sup>	a = 5.4376, b = 16.3775, c = 5.4169	-
ZnAlWBiO-2	a = 3.2157, c = 5.1683	a = 8.0261	a = 4.6579, b = 5.6797, c = 4.9057, β = 90.284 <sup>0</sup>	a = 5.4173, b = 16.3165, c = 5.3839	-
ZnAlWBiO-3	-	a = 8.0214	a = 4.6314, b = 5.6563, c = 4.8951, β = 90.160 <sup>0</sup>	a = 5.4077, b = 16.2493, c = 5.3723	-
ZnAlWBiO-4	-	a = 8.0576	a = 4.6723, b = 16.3035, c = 5.4029, β = 90.390 <sup>0</sup>	a = 5.4406, b = 16.3035, c = 5.4029	-
ZnAlWBiO-5	-	a = 8.0689	-	a = 5.4450, b = 16.4129, c = 5.4286	a = 5.3957, b = 5.4479, c = 23.6619

On the basis of the obtained diffraction patterns as well as the analysis of the phase composition, the volume contributions of various phases in the composition of ceramics were determined depending on the Bi<sub>2</sub>O<sub>3</sub> dopant concentration. The results of this analysis are presented in Figure 4. To determine the phase content, the Rietveld method was used and the calculation of Formula (1),

$$V_{\text{admixture}} = \frac{RI_{\text{phase}}}{I_{\text{admixture}} + RI_{\text{phase}}}, \quad (1)$$

where  $I_{\text{phase}}$  is the average integrated intensity of the main phase of the diffraction line,  $I_{\text{admixture}}$  is the average integrated intensity of the additional phase, and  $R$  is the structural coefficient equal to 1.45.

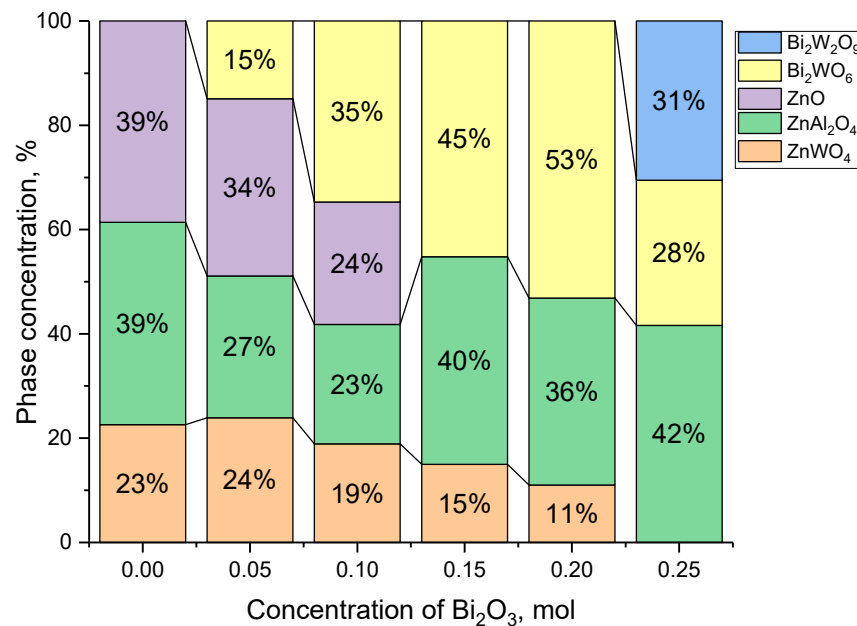


Figure 4. Results of evaluation of the volume contributions of phases to the composition of ceramics.



The general view of the presented results of changes in the volume fractions of the contributions of various phases to the composition of ceramics depending on the concentration of  $\text{Bi}_2\text{O}_3$  can be characterized by the following scheme of phase transformations:  $\text{ZnO}/\text{ZnAl}_2\text{O}_4/\text{ZnWO}_4 \rightarrow \text{ZnO}/\text{ZnAl}_2\text{O}_4/\text{ZnWO}_4/\text{Bi}_2\text{WO}_6 \rightarrow \text{ZnAl}_2\text{O}_4/\text{ZnWO}_4/\text{Bi}_2\text{WO}_6 \rightarrow \text{ZnAl}_2\text{O}_4/\text{Bi}_2\text{WO}_6/\text{Bi}_2\text{W}_2\text{O}_9$ . According to this scheme, an increase in the concentration of the  $\text{Bi}_2\text{O}_3$  dopant leads to the formation of orthorhombic phases similar to complex oxides containing bismuth, which leads to the displacement of the  $\text{ZnO}$  phase at a  $\text{Bi}_2\text{O}_3$  concentration of 0.10 mol, and the subsequent transformation of the  $\text{ZnWO}_4$  phase into the  $\text{Bi}_2\text{WO}_6$  and  $\text{Bi}_2\text{W}_2\text{O}_9$  phases. Such changes in the phase composition lead to a change not only in the structural parameters, but also in the dislocation density and the appearance of boundary effects associated with different grains, which are clearly visible when mapping the obtained samples.

### 3.3. Analysis of Optical Properties

Figure 5 shows the results of changes in the optical transmission spectra of the studied glass ceramics depending on the concentration of the  $\text{Bi}_2\text{O}_3$  dopant. The general view of the obtained dependences is characterized by a high bandwidth in the region characteristic of the visible range (400–700 nm) and a slight decrease in the throughput intensity in the range characteristic of the near IR range (above 750 nm). At the same time, in the region of 350–400 nm, which is characteristic of the fundamental absorption edge, a shift of the spectra is observed, which is characteristic of a change in the electronic distribution and band gap.

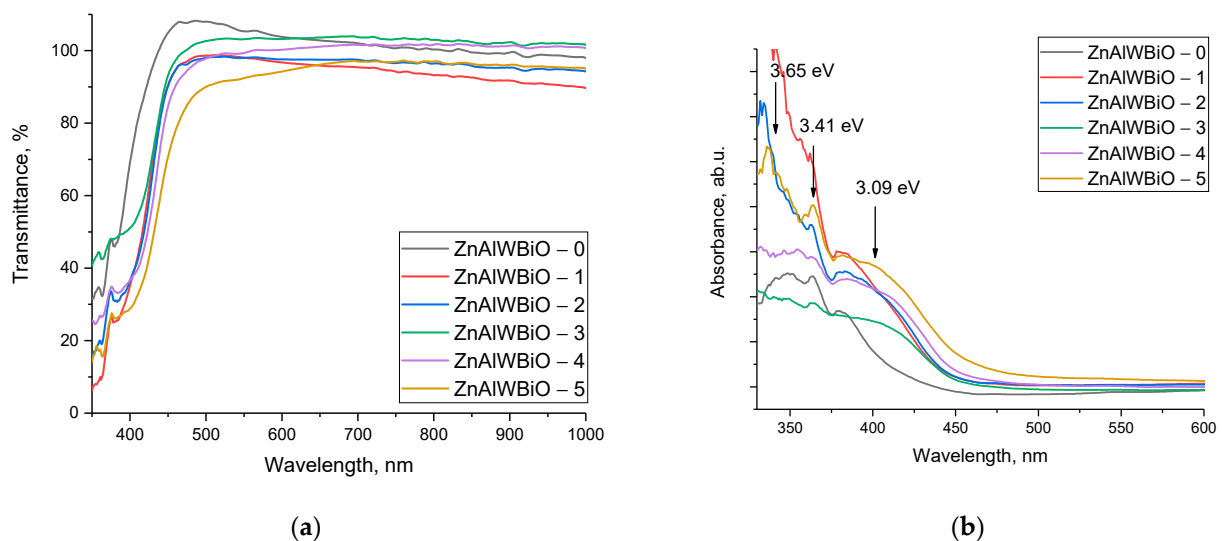


**Figure 5.** Results of the transmission spectra of the studied glasses as a function of the  $\text{Bi}_2\text{O}_3$  concentration: (a) transmission spectra; (b) absorption spectra.

It was found that a change in the phase composition of ceramics leads to a slight decrease in the transmittance in the region characteristic of visible light (400–700 nm) as well as a shift in the fundamental absorption edge. The decrease in transmission intensity is no more than 5–7%.

The absorption spectra presented in Figure 5b indicate the formation of additional absorption bands at 3.65 eV, 3.41 eV, and 3.09 eV, the presence of which is due to a change in the electron density as well as the formation of additional absorption centers associated with the processes of phase transformations.

Based on the obtained UV-V is spectra, the band gap values for the studied ceramics were calculated by constructing Tauc plots. The results of the construction are shown in Figure 6. The tangential dashed lines determine the value of the band gap, as well as its change depending on the phase composition of the ceramics and the concentration of the

dopant. The general form of the changes obtained indicates a shift in the fundamental absorption edge, which indicates a change in the electron density and band gap of the obtained ceramics. These changes are due to the processes of phase transformations, which were established by X-ray phase analysis.

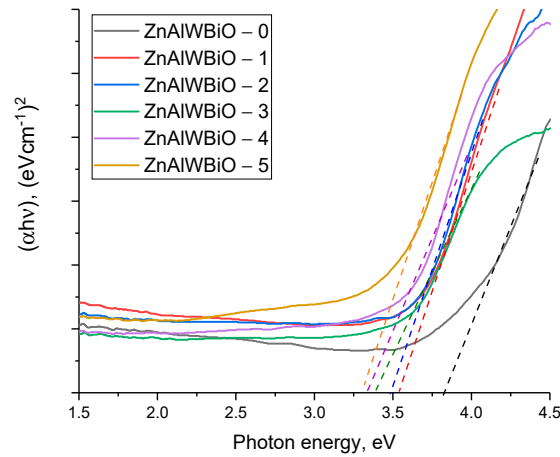


**Figure 6.** Results of Tauc plots that determine the change in the value of the fundamental absorption edge and the band gap.

Table 4 presents the results of determining the band gap ( $E_g$ ) and the linear refractive index ( $n^{optical}$ ), which were calculated by analyzing the data obtained in Figure 6 using Formulas (2) and (3).

$$\alpha = A(h\nu - E_g)^{1/2} \quad (2)$$

where  $A$  is a constant, and  $h\nu$  is the photon energy.

$$\frac{\left[ \left( n^{optical} \right)^2 - 1 \right]}{\left[ \left( n^{optical} \right)^2 + 2 \right]} = 1 - \sqrt{\frac{E_g}{20}} \quad (3)$$

**Table 4.** Band gap and linear refractive index data.

Sample	$E_g$ , eV	$n^{optical}$
ZnAlWBio-0	3.826	2.204
ZnAlWBio-1	3.539	2.265
ZnAlWBio-2	3.465	2.281
ZnAlWBio-3	3.403	2.296
ZnAlWBio-4	3.338	2.311
ZnAlWBio-5	3.289	2.323

Analyzing the obtained dependencies of changes in the magnitude of the band gap and the linear refractive index, we can draw the following conclusions. The displacement of the ZnO hexagonal phase from the structure leads to a decrease in the band gap, as well as the formation of three additional absorption bands, the presence of which indicates changes in the optical absorbing properties of ceramics. At the same time, the formation of orthorhombic  $\text{Bi}_2\text{WO}_6$  and  $\text{Bi}_2\text{W}_2\text{O}_9$  phases leads to an increase in the refractive index, which is due to effects associated with a change in the dislocation and defect density in the ceramic structure.

### 3.4. Measurement of Strength Properties

One of the important characteristics for radiation-resistant protective materials is their resistance to external mechanical influences, including compression, damage or external impacts, that can lead to the formation of microcracks or chips, which can lead to the destruction of the protective material and affect its operating conditions. In this case, as is known, the mechanical strength and resistance to cracking have a pronounced dependence on the phase composition of the samples, as well as dimensional factors associated with grain sizes, boundary effects, and dislocation density. These factors, the change of which is directly related to the processes of phase transformations with a change in the concentration of the initial components, can have a significant effect on the hardening of ceramics and an increase in their resistance to external influences.

Figure 7 shows the results of changes in the strength characteristics of the synthesized ceramics depending on the  $\text{Bi}_2\text{O}_3$  dopant concentration, which reflect the effects of hardening with a change in the phase composition of the samples under study.

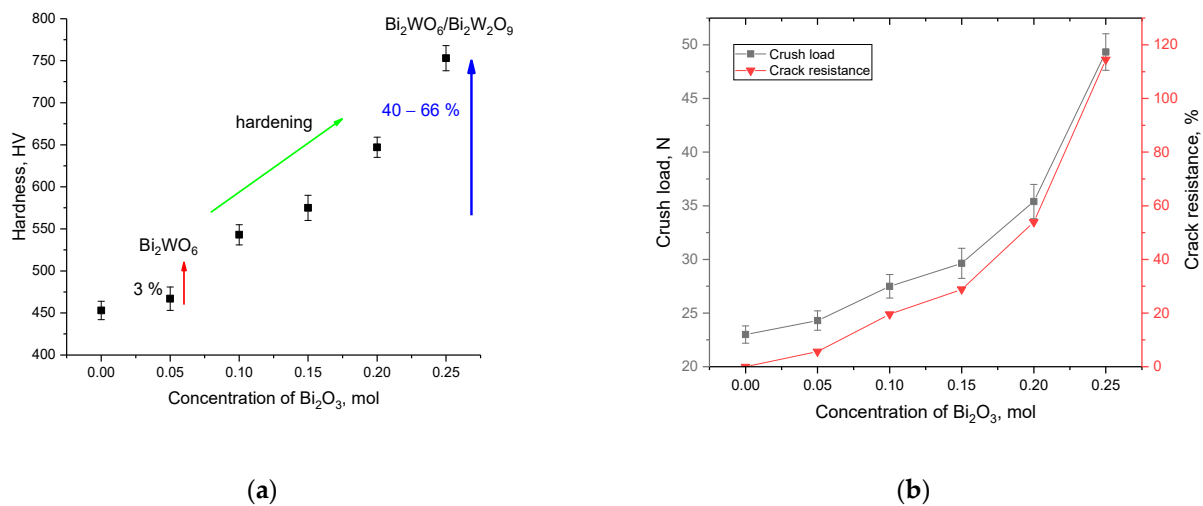


**Figure 7.** (a) Results of changes in the hardness and hardening of ceramics depending on the concentration of the  $\text{Bi}_2\text{O}_3$  dopant; (b) results of the change in the crack resistance value of ceramics depending on the  $\text{Bi}_2\text{O}_3$  dopant concentration.

Analyzing these changes in hardness, it was found that with the formation of the  $\text{Bi}_2\text{WO}_6$  phase in the structure and the partial displacement of the  $\text{ZnO}$  phase at low concentrations of the  $\text{Bi}_2\text{O}_3$  dopant (no more than 0.05 mol), the strengthening effect is no more than 3%. At the same time, with an increase in the concentration of the  $\text{Bi}_2\text{O}_3$  dopant above 0.10 mol, it was found that the strengthening effect is more than 10–20% and increases with a change in the phase composition. In turn, the formation of the  $\text{Bi}_2\text{WO}_6$  and  $\text{Bi}_2\text{W}_2\text{O}_9$  phases leads to the strengthening of ceramics by a factor of more than 1.5 compared to undoped samples, which indicates a high efficiency of hardening.

During analysis of the data for determination of the crack resistance, the results of which are presented in Figure 7b, a similar dependence of the change in the crack resistance value under single compression on the change in the phase composition of the ceramics, as well as an increase in the contribution of the  $\text{Bi}_2\text{WO}_6$  phase, is established. At the same time, the formation of the  $\text{Bi}_2\text{W}_2\text{O}_9$  phase leads to a more than twofold increase in resistance to cracking and an increase in resistance to the maximum withstand load.

Figure 8 shows the results of changes in the density of ceramics as well as an assessment of the contributions of dislocation density and boundary effects to the strengthening of ceramics and an increase in resistance to external influences.

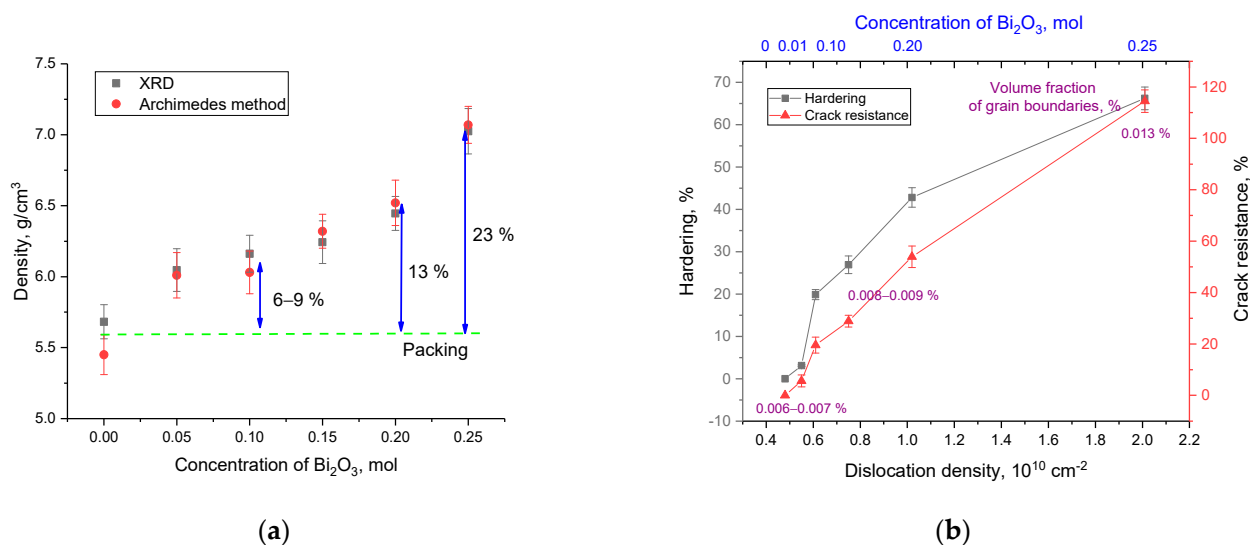


**Figure 8.** (a) Results of changes in the density of ceramics; (b) Results of ceramic hardening data depending on the change in dislocation density.

As can be seen from the presented data on the change in density, which was measured by two methods (X-ray diffraction and the method of Archimedes), a change in the phase composition leads to an increase in the density of ceramics as well as its compaction, the maximum value of which is more than 20%. At the same time, it should be noted that the density measurement data determined by two independent methods are in good agreement, which indicates a low porosity of the ceramics. The results of hardening have a pronounced dependence on changes in the dislocation density of ceramics and boundary effects, the increase in which is associated with a decrease in grain size with a change in the phase composition of ceramics. At the same time, the greatest strengthening effect is manifested with an increase in the dislocation density by more than 2–3 times, compared with the original samples. In this case, it can be said with certainty that a change in the phase composition of ceramics at high concentrations of the Bi<sub>2</sub>O<sub>3</sub> dopant leads to the strengthening of ceramics as well as an increase in their resistance to external influences and mechanical damage. In the future, these results can be used in the design of protective coatings and materials based on these compounds.

#### 4. Conclusions

During the studies performed using the method of X-ray phase analysis, the dynamics of phase transformations was established depending on the Bi<sub>2</sub>O<sub>3</sub> concentration, which consists in the formation of orthorhombic Bi<sub>2</sub>WO<sub>6</sub> and Bi<sub>2</sub>W<sub>2</sub>O<sub>9</sub> phases, as well as the displacement of the ZnO phase. The general trend of phase transformations depending on the Bi<sub>2</sub>O<sub>3</sub> dopant concentration can be written as follows: ZnO/ZnAl<sub>2</sub>O<sub>4</sub>/ZnWO<sub>4</sub> → ZnO/ZnAl<sub>2</sub>O<sub>4</sub>/ZnWO<sub>4</sub>/Bi<sub>2</sub>WO<sub>6</sub> → ZnAl<sub>2</sub>O<sub>4</sub>/ZnWO<sub>4</sub>/Bi<sub>2</sub>WO<sub>6</sub> → ZnAl<sub>2</sub>O<sub>4</sub>/Bi<sub>2</sub>WO<sub>6</sub>/Bi<sub>2</sub>W<sub>2</sub>O<sub>9</sub>. At the same time, it was found that the formation of orthorhombic phases leads to an increase in the density of ceramics as well as a change in the dislocation density, which has a significant effect on the change in the strength properties of ceramics. During determination of the optical characteristics, it was found that a change in the phase composition of ceramics leads to a decrease in the band gap as well as the formation of additional absorption bands, which indicates an increase in the absorption capacity of ceramics. An analysis of the mechanical and strength properties of the samples under study showed that a change in the phase composition of ceramics leads to a more than 1.5–2-fold increase in resistance to external influences, which is due to both a change in the density of ceramics and strengthening effects due to changes in the dislocation density.



Further studies in this direction will be aimed at studying the effectiveness of the use of the obtained ceramics as shielding materials and protective coatings against the negative effects of ionizing radiation.

**Author Contributions:** Conceptualization, A.L.K., D.B.B. and A.S.S.; methodology, M.V.Z. and A.L.K.; formal analysis, M.V.Z. and A.L.K.; investigation, M.V.Z., A.S.S. and A.L.K.; resources, A.L.K.; writing—original draft preparation, review, and editing, D.B.B. and A.L.K.; visualization, A.L.K.; supervision, A.L.K. All authors have read and agreed to the published version of the manuscript.

**Funding:** This research was funded by the Science Committee of the Ministry of Education and Science of the Republic of Kazakhstan (No. AP13068151).

**Institutional Review Board Statement:** Not applicable.

**Informed Consent Statement:** Not applicable.

**Data Availability Statement:** Not applicable.

**Conflicts of Interest:** The authors declare no conflict of interest.

## References

1. Di Trolio, R.; Di Lorenzo, G.; Fumo, B.; Ascierio, P.A. Cosmic radiation and cancer: Is there a link? *Future Oncol.* **2015**, *11*, 1123–1135. [[CrossRef](#)] [[PubMed](#)]
2. Lochard, J.; Bartlett, D.T.; Rühm, W.; Yasuda, H.; Bottollier-Depois, J.F. ICRP publication 132: Radiological protection from cosmic radiation in aviation. *Ann. ICRP* **2016**, *45*, 5–48. [[CrossRef](#)]
3. Blachowicz, T.; Ehrmann, A. Shielding of Cosmic Radiation by Fibrous Materials. *Fibers* **2021**, *9*, 60. [[CrossRef](#)]
4. Elsafi, M.; El-Nahal, M.A.; Alrashedi, M.F.; Olarinoye, O.I.; Sayyed, M.I.; Khandaker, M.U.; Abbas, M.I. Shielding properties of some marble types: A comprehensive study of experimental and XCOM results. *Materials* **2021**, *14*, 4194. [[CrossRef](#)]
5. Kotomin, E.A.; Popov, A.I.; Stashans, A. A novel model for F+ to F photoconversion in corundum crystals. *J. Phys. Condens. Matter* **1994**, *6*, L569–L573. [[CrossRef](#)]
6. Zhong, W.H.; Sui, G.; Jana, S.; Miller, J. Cosmic radiation shielding tests for UHMWPE fiber/nano-epoxy composites. *Compos. Sci. Technol.* **2009**, *69*, 2093–2097. [[CrossRef](#)]
7. Millers, D.; Grigorjeva, L.; Chernov, S.; Popov, A.I.; Lecoq, P.; Auffray, E. The temperature dependence of scintillation parameters in PbWO<sub>4</sub> crystals. *Phys. Status Solidi B* **1997**, *203*, 585–589. [[CrossRef](#)]
8. Ciesielska-Wróbel, I.; Grabowska, K. Estimation of the EMR shielding effectiveness of knit structures. *Fibres Text. East. Eur.* **2012**, *20*, 53–60.
9. Al-Hadeethi, Y.; Sayyed, M.I. BaO–Li<sub>2</sub>O–B<sub>2</sub>O<sub>3</sub> glass systems: Potential utilization in gamma radiation protection. *Prog. Nucl. Energy* **2020**, *129*, 103511. [[CrossRef](#)]
10. Eglitis, R.I.; Purans, J.; Gabrusenoks, J.; Popov, A.I.; Jia, R. Comparative ab initio calculations of ReO<sub>3</sub>, SrZrO<sub>3</sub>, BaZrO<sub>3</sub>, PbZrO<sub>3</sub> and CaZrO<sub>3</sub> (001) surfaces. *Crystals* **2020**, *10*, 745. [[CrossRef](#)]
11. Sayyed, M.I.; Akman, F.; Kumar, A.; Kaçal, M.R. Evaluation of radioprotection properties of some selected ceramic samples. *Results Phys.* **2018**, *11*, 1100–1104. [[CrossRef](#)]
12. Hannachi, E.; Sayyed, M.I.; Slimani, Y.; Elsafi, M. Experimental investigation on the physical properties and radiation shielding efficiency of YBa<sub>2</sub>Cu<sub>3</sub>Oy/M@M<sub>3</sub>O<sub>4</sub> (M = Co, Mn) ceramic composites. *J. Alloys Compd.* **2022**, *904*, 164056. [[CrossRef](#)]
13. Asal, S.; Erenturk, S.A.; Hacıyakupoglu, S. Bentonite based ceramic materials from a perspective of gamma-ray shielding: Preparation, characterization and performance evaluation. *Nucl. Eng. Technol.* **2021**, *53*, 1634–1641. [[CrossRef](#)]
14. Kasenov, B.K.; Kasenova, S.B.; Sagintaeva, Z.I.; Nukhuly, A.; Turtubaeva, M.O.; Bekturganov, Z.S.; Issabaeva, M.A. Synthesis and X-ray investigation of novel nanostructured copper-zinc manganites of lanthanum and alkali metals. *Eurasian Phys. Tech. J.* **2021**, *18.1*, 29–33. [[CrossRef](#)]
15. Kacal, M.R.; Akman, F.; Sayyed, M.I. Investigation of radiation shielding properties for some ceramics. *Radiochim. Acta.* **2019**, *107*, 179–191. [[CrossRef](#)]
16. Kavaz, E.; EL\_Agawany, F.I.; Tekin, H.O.; Perişanoğlu, U.; Rammah, Y.S. Nuclear radiation shielding using barium borosilicate glass ceramics. *J. Phys. Chem. Solids* **2020**, *142*, 109437. [[CrossRef](#)]
17. Alotaibi, B.M.; Alotiby, M.; Kumar, A.; Mahmoud, K.A.; Sayyed, M.I.; Al-Yousef, H.A.; Al-Hadeethi, Y. Gamma-ray shielding, physical, and structural characteristics of TeO<sub>2</sub>–CdO–PbO–B<sub>2</sub>O<sub>3</sub> glasses. *Opt. Mater.* **2021**, *119*, 111333. [[CrossRef](#)]
18. Obaid, S.S.; Sayyed, M.I.; Gaikwad, D.K.; Pawar, P.P. Attenuation coefficients and exposure buildup factor of some rocks for gamma ray shielding applications. *Radiat. Phys. Chem.* **2018**, *148*, 86–94. [[CrossRef](#)]
19. Sayyed, M.I.; AlZaatreh, M.Y.; Dong, M.G.; Zaid, M.H.M.; Matori, K.A.; Tekin, H.O. A comprehensive study of the energy absorption and exposure buildup factors of different bricks for gamma-rays shielding. *Results Phys.* **2017**, *7*, 2528–2533. [[CrossRef](#)]
20. Hannachi, E.; Sayyed, M.I.; Almuqrin, A.H.; Mahmoud, K.G. Study of the structure and radiation-protective properties of yttrium barium copper oxide ceramic doped with different oxides. *J. Alloys Compd.* **2021**, *885*, 161142. [[CrossRef](#)]

21. Ataalla, M.; Milanova, M.; Aleksandrov, L.; Iordanova, R.; Staneva, A.; Dimitriev, Y. Glass formation and structure of glasses in the ZnO–WO<sub>3</sub>–La<sub>2</sub>O<sub>3</sub>–Al<sub>2</sub>O<sub>3</sub> system. *J. Chem. Technol. Metall.* **2015**, *50*, 423–428.
22. Alomairy, S.; Alrowaili, Z.A.; Kebaili, I.; Wahab, E.A.; Mutuwong, C.; Al-Buriahi, M.S.; Shaaban, K.S. Synthesis of Pb<sub>3</sub>O<sub>4</sub>-SiO<sub>2</sub>-ZnO-WO<sub>3</sub> glasses and their fundamental properties for gamma shielding applications. *Silicon* **2022**, *14*, 5661–5671. [[CrossRef](#)]
23. Dimitriev, Y.; Iordanova, R.; Milanova, M.; Bachvarova-Nedelcheva, A.; Hassan, M.; Abdallah, M. Crystallisation of ZnO from supercooled melts and glasses. *Phys. Chem. Glasses-Eur. J. Glass Sci. Technol. Part B* **2012**, *53*, 254–263.